Processing of Ultrasonic Array Signals for Characterizing Defects. Part II: Experimental Work

Guillermo Rus, *Member, IEEE*, Shi-Chang Wooh, *Member, IEEE*, and Rafael Gallego, *Member, IEEE*

***Abstract*—This is Part II of the two-part paper aimed at integrating the numerical synthesis and experimental investigation of the ultrasonic wave propagation model for quantitative nondestructive evaluation. The first part of the paper focused on synthesizing and predicting measured signals using the boundary element method and the deconvolution technique based on the comparison between the signals obtained from defective and undamaged (reference) specimens.**

In the second part, we present an inversion technique which allows us to obtain the position and size of the defect. The inversion scheme is processing the frequency domain information rather than time-domain time-of-flights or vibration eigenmodes. This technique is tested experimentally for the case of a side-drilled hole with a non-trivial location in terms of standard pulse-echo techniques. It is shown that the scheme is particularly effective when the information of the defect is masked by other predominant signal components.

I. Introduction

Ultrasonic wave propagation phenomena have been traditionally analyzed by some complex and limited analytical solutions, e.g., Viktorov [1], Miler and Pursey [2], Pao and Mow [3], or Graff [4]. An inverse problem can be solved by deriving simplified relationships between the excitation and response (which can be expressed by a transfer function), which substitutes the solution of a direct problem (e.g., Wooh *et al.* [5] or Boström *et al.* [6], [7]).

Another way to solve an inverse problem is to use the forward problem to find its solutions by an iterative search scheme (e.g., Wirdelius [8]). Our approach, which falls in this category, is to seek the solutions that minimize the discrepancy between the predicted model and actual measurements.

The boundary element method (BEM) was initially used by a host of investigators [9]–[11] to numerically detect simulated defects for specimens with simple geometries, using such iterative schemes. Their works were followed by a group of investigators in the past decades [12]–[14]. In our work, the methods developed by Gallego, Rus, and Suárez [15]–[17], based on minimizing the error between the predicted and actual measurements, are adopted and further developed.

The issue of probability of detection (POD) is an important question addressed by the statistics science. Liu *et al.* [18] discussed the identifiability, which is the relationship between the number of measurements and the degrees of freedom to establish a necessity condition for detection. Tarantola *et al.* [19] investigated the inversion problem by formulating the probabilistic functions and introducing the probability density function in their model to obtain a non-single valued output for the parameters. They also introduced the concept of *a priori* parametric knowledge to explain the robustness of the inversion process.

In an inverse problem, we seek a solution for a set of parameters that minimize the difference between the predicted and the actual measurements. In dynamics, the parameters such as mode shape or deformation have been widely used as the parameters to seek. Some reciprocal techniques [20] have also been successfully tested to find the load vector that gives an unchanged response. Our approach compares the response of a damaged specimen with that of an undamaged (reference) specimen. In our work, we use a synthetic array [21], [22] to solve the problems associated with the multiplication of the cost by numerous simultaneous transducers as well as cross-talks between the channels of a phased array.

A discussion of how sensitive this boundary integral equation inverse problem solution approach is to variations in material properties, measurement noise and geometrical variations is provided by Rus *et al.* [23], [24]. They concluded that robust convergence after quantifying the effect of errors in geometry, mechanical constants, frequency, and measurements, for a set of parametrizations of arbitrarily shaped defects, provided a sufficient number of measurements and frequency range as well as a proper parametrization.

II. Inverse Procedure

A. Parametrization

In an inverse problem, we seek information such as the size and orientation of defects based on the known for-

Manuscript received June 5, 2006; accepted May 25, 2007. We gratefully acknowledge the Fulbright Foundation and the Ministerio de Educación, Cultura y Deporte for the postdoctoral fellowship FU2002-0442 supporting this work.

R. Guillermo and S.-C. Wooh are with the NDE Laboratory, Department of Civil and Environmental Engineering, Massachusetts Institute of Technology, Cambridge, MA 02139 (e-mail: grus@ugr.es).

R. Gallego is with the Department of Structural Mechanics, University of Granada, Granada, Spain.

Digital Object Identifier 10.1109/TUFFC.2007.509

ward problem. Finding such information could be possible by first introducing *a priori* information and setting the scope by means of proper parametrization. The issues related to the parametrization could be complicated due to the complexity of the relationships between many hypothetical arguments. Many inverse problems are ill-posed: Solutions may not exist, there may exist multiple solutions, or they could be unstable or non-converging. This is true especially when we are dealing with a full set of parameters. It is thus common to characterize the system using a set of parameters (p_g) with a reduced number of variables (g). Choosing the appropriate parameters is a critical step influencing the convergence, the sensitivity of the result, and the decoupling of their dependence from the measurements. The simplest and most robust form is a two-parameter system in seeking the location of the defects: the depth (p_1) and diameter (p_2) of the side-drilled hole defect.

B. Residual

A residual vector $\mathbf{R}$ is introduced in order to quantify the discrepancy between the ideal measurements and theoretical predictions. While the prediction is based on a set of g parameters p_g, the ideal measurement data can be denoted by a corresponding set p_g^r, where the superscript r denotes a real defect.

The main contribution at this point is that the information to be used for the definition of the residual is not the straightforward output signal $s^{(O)}(t)$, but the response of the model $h^{(TR)}(t)$ or $H^{(TR)}(\omega)$ (the convention of capital letters for frequency domain is adopted). It is analyzed in the frequency domain. Recall that this magnitude is defined in (1), where p_g^r are the parameters for the real defect, $\Lambda = \Lambda(\omega)$ is the frequency domain form of the random noise process $\lambda(t)$, and Z is the amplitude compensation variable $z = z^{(TR)}(t)$ in the time domain,

$$\hat{H}_{mn}^{(TR)}(p_g^r, Z) = \frac{1}{Z} H_{mn}^{(TR)} + N_{mn}^{(TR)} \Lambda. \tag{1}$$

The predicted data are computed for a trial value of the parameters p_g, $\tilde{H}_{rej}^{(TR)}(p_g)$, that is defined as

$$\begin{aligned} \tilde{H}_{mn}^{(TR)}(p_g) &= \hat{H}_{mn}^{(TR)}(p_g^r, Z) + D_{mn}(p_g, Z) + N_{mn}^{(TR)} \Lambda \\ &= \frac{1}{Z} H_{mn}^{(TR)} + D_{mn}(p_g, Z). \end{aligned} \tag{2}$$

It approaches the ideal measurement defined above. In (2), the difference between the ideal ($\hat{H}^{(TR)}$) and computed ($\tilde{H}^{(TR)}$) models—numerical and model errors—is added as part of the noise ($N^{(TR)}$) in the sequel. Now we define the residual vector $\mathbf{R}$ in terms of the above discrepancy D as

$$\begin{aligned} \mathbf{R}(p_g, Z) = R_{mn}(p_g, Z) &= W\left[D_{mn}(p_g, Z)\right] \\ &= W\left[\tilde{H}_{mn}^{(TR)}(p_g) - \frac{1}{Z} H_{mn}^{(TR)}\right]. \end{aligned} \tag{3}$$

A filter $W = W(\omega)$ is introduced to weight relevant frequencies and eliminate others. This can be used for filtering the noise (see Rus *et al.* [24]). It is important to note that the residual $\mathbf{R}$ defined in terms of the difference between the trial and experimental transfer functions is equivalent to the discrepancy $\mathbf{R}'$ between the relative differences of undamaged and defective specimens, except for a factor $(G/\overset{\circ}{S}{}_{mn}^{(O)})$, where $G = G(\omega)$ is the frequency domain form of $g(t)$:

$$\begin{aligned} R'_{mn} &= \frac{G}{\overset{\circ}{S}{}_{mn}^{(O)}} R_{mn} \\ &= W\left[\left(\frac{S_{mn}^{(O)} - \overset{\circ}{S}{}_{mn}^{(O)}}{\overset{\circ}{S}{}_{mn}^{(O)}}\right) - \left(\frac{\tilde{H}_{mn}^{(TR)}(p_g)\frac{G}{G_{mn}} - \overset{\circ}{\tilde{H}}{}_{mn}^{(TR)}}{\overset{\circ}{\tilde{H}}{}_{mn}^{(TR)}}\right)\right]. \end{aligned} \tag{4}$$

C. Undamaged Specimen for Compensation

Referring back to (2) for the undamaged specimen (where D_{mn} vanishes by definition), it is possible to include the amplitude factor Z inside G. Provided that Z is the same for the undamaged and the defective tests, the factor is effectively eliminated for the entire formulation:

$$\overset{\circ}{\tilde{H}}{}_{mn}^{(TR)} = \frac{1}{Z} \overset{\circ}{H}{}_{mn}^{(TR)} = \frac{1}{Z} \left(G'\right)^{-1} \overset{\circ}{S}_{mn}, \quad G = ZG'. \tag{5}$$

D. Cost Functional

A cost functional J is defined in terms of the residual $\mathbf{R}$ in quadratic sense, which is basically a least square. This definition is meaningful from the statistical point of view, as well as from a space theory, since it minimizes the distances in an euclidean sense. The cost functional is hence defined as in (7) for the case of the discrete frequency domain:

$$\begin{aligned} J &= \frac{1}{2} \mathbf{R}^T \overline{\mathbf{R}} = \frac{1}{2} \|\mathbf{R}\|^2 \\ J(p_g, z) &= \frac{1}{2} \sum_{j=-\infty}^{+\infty} R_{mn}(p_g, z, \omega_j) \overline{R}_{mn}(p_g, z, \omega_j), \end{aligned} \tag{6}$$

where T stands for the transpose in vectorial notation and $\overline{\mathbf{R}}$ means the conjugate of the complex magnitude $\mathbf{R}$. In the following, the proof of equivalence between time- and frequency-domain definitions of the cost functional J is made. Moreover, this proof provides a consistent definition of J in which two signals $f(t)$ and $g(t)$ ($t = 0 - T$) are compared. The functional is weighted by a generic function $w(t)$:

$$
\begin{aligned}
2TJ &= \int_0^T \left[w(t) * (f(t) - g(t))\right]^2 dt \\
&= \int_0^T \left[\sum_{j=-\infty}^{+\infty} W_j (F_j - G_j) e^{\frac{2\pi i j t}{T}}\right]^2 dt \\
&= \int_0^T \sum_{j,k=-\infty}^{+\infty} W_j (F_j - G_j) W_k (F_k - G_k) e^{\frac{2\pi i (j+k) t}{T}} dt \\
&= \sum_{j=-\infty}^{+\infty} W_j (F_j - G_j) W_{-j} (F_{-j} - G_{-j}) \\
&= \sum_{j=-\infty}^{+\infty} W_j (F_j - G_j) \overline{W}_j (\overline{F}_j - \overline{G}_j) \\
&= \sum_{j=-\infty}^{+\infty} \left|W_j\right|^2 \left|(F_j - G_j)\right|^2 = 2TJ,
\end{aligned} \tag{7}
$$

where

$$
\overline{F}_j = \int_0^1 \overline{f}(t) \overline{e^{\frac{2\pi i j t}{T}}} dt = \int_0^1 f(t) e^{\frac{-2\pi i j t}{T}} dt = F_{-j}. \tag{8}
$$

The extension to the case of a synthetic array of impactors m or receivers n, which can be weighted by v_{mn} in which $R'_{mn}(t) = f(t) - g(t)$, applied to the previously defined residual $\mathbf{R}$, and converted to the discrete time and frequency domains yields

$$
\begin{aligned}
2TJ &= \sum_{m,n} v_{mn}^2 J_{mn} \\
&= \frac{T}{N} \sum_{m,n} \int_0^T \left[w(t) * v_{mn} R'_{mn}(t)\right]^2 dt \\
&= \frac{T}{N^2} \sum_{m,n,j} \left|v_{mn} W(\omega_j)\right|^2 \left|R'_{mn}(t)\right|^2.
\end{aligned} \tag{9}
$$

E. Fitness Function

An optimization algorithm is used to find the values of the set of parameters included in vector p_g that minimize the discrepancy between the numerically predicted response and the measurement. From (10) a fitness function f is defined to be maximized:

$$
f(p_g) = -\log(J(p_g) + \epsilon), \tag{10}
$$

where $J(p_g)$ is the cost functional and ϵ is a small constant introduced to avoid numerical errors, and whose main condition is to be larger than the round-off errors of computational arithmetics introduced in J.

This fitness function was chosen to give better results when applied to certain optimization techniques such as genetic algorithms (see Rus *et al.* [25]).

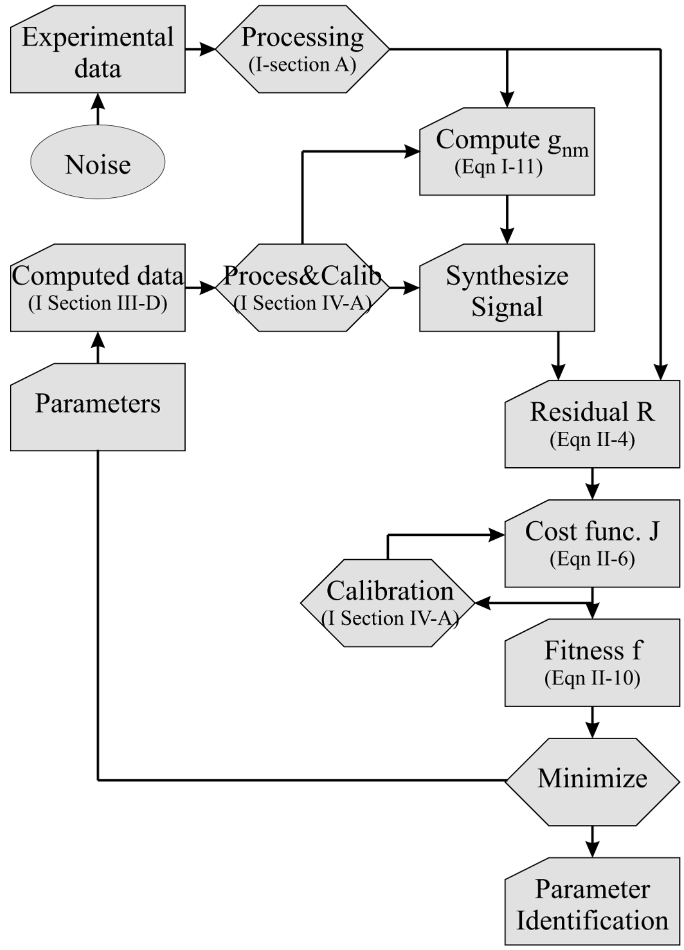

Fig. 1. Flow chart of the inverse problem solution from experimental data.

III. Implementation

A. Flow Chart

The theory described above is implemented for evaluating a defect in a specimen using the recorded output signal as described in the flow chart in Fig. 1.

1. **Preprocessing:** process experimental signal (described in Part I).
2. **Calibration:** synthesize a signal (described in Part I).
3. **Inversion:** An iterative maximization algorithm for the fitness function f carries out the following operations at each iteration, in which p_g is varied according to the chosen maximization algorithm. The proposed test is limited to a uniformly spaced search for each parameter.
   a) Compute $\tilde{H}_{mn}^{(TR)}$ for a defect defined by parameters p_g, using the BEM. Each term j is obtained from the solution of a single frequency. The numerical technique, the boundary conditions, and the relationship between the signal and the response ($s_m^{(T)}(t) = q_i(\Gamma_m, t) n_i$ and $s_{mn}^{(R)}(t) = \int_{\Gamma_n} u_i(\Gamma, t) d\Gamma n_i$) were explained previously.

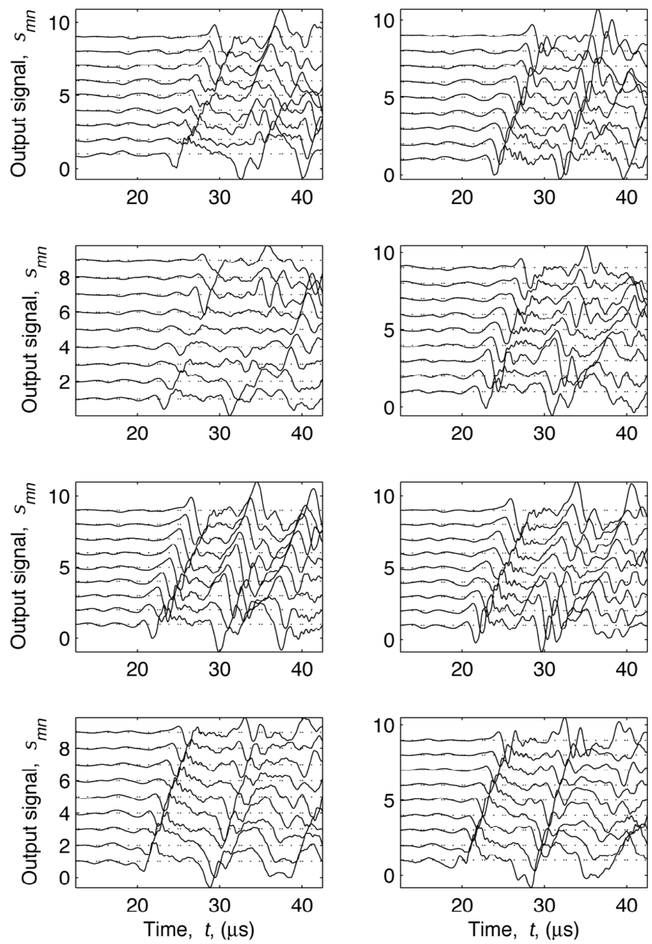

Fig. 2. Residual between experimental and synthesized signal at all eight receivers from all eight transmitters. Case with no defect.

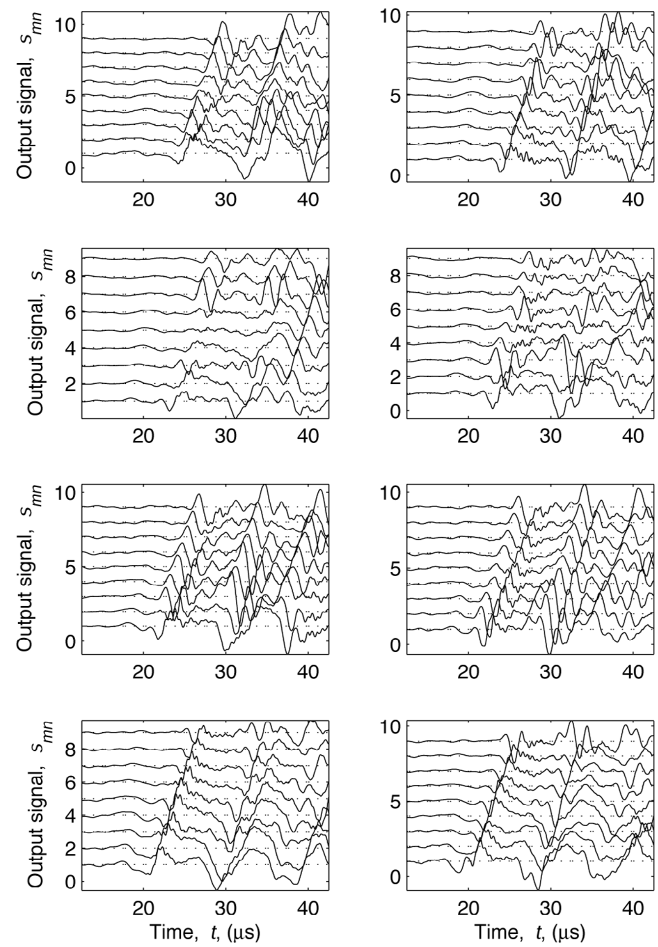

Fig. 3. Residual between experimental and synthesized signal at all eight receivers from all eight transmitters. Case with defect.

b) Resample $\tilde{h}_{mn}^{(TR)}(t)$ according to the calibrated value of α.
c) Generate experimental transfer function $h_{mn}^{(TR)}(t) = g^{-1}(t) * s_{mn}^{(O)}$.
d) Compute the residual $\mathbf{R} = h_{mn}^{(TR)}(t) - \tilde{h}_{mn}^{(TR)}(t)$.
e) Join the first and last points of the residual $\mathbf{R}$ by a linear transition during the last 2.5 μs.
f) Multiply by the weight function $w(t)$.
g) Compute the cost functional $J = \frac{1}{2N}\sum_{i=1}^{N}(\mathbf{R})^2$, and the fitness function f.

B. Methodology

The formulas developed in Part I are used to analyze the signals obtained from an aluminum specimen with a subsurface defect. Due to the high cost for three-dimensional BEM, we consider only a two-dimensional problem (Rus [26]), in which the problem is simplified by the plane strain assumption. In order to improve the directivity and frequency responses of the transmitting and receiving transducers, we used specially designed contact transducers [27], which also improve the repeatability of experiments.

The key factor for a well-behaving inverse problem is to control the pressure acting on the transducers so that the variations of pressure from transducer to transducer are minimal. For this purpose, we have fabricated a special fixture using gravitational pressure, producing consistent forces for each pulse event. In addition, a spike pulse function is used as input in order to produce broadband frequency content that provides rich information.

IV. Experimental Results

The top half of Fig. 8 in Part I shows the signals obtained from an experiment and the synthesized signal. These experiments are repeated for both the reference sample and the specimen with the defect in the bottom half of the same figure. Note that the signals are similar because the main contribution consists of a surface wave, which is not affected by the presence of the defect. It can be argued that the proposed inversion technique is robust enough to identify the defect from the underlying difference.

Figs. 2 and 3 show the residual $\mathbf{R}$ in the time domain for all of the receivers and transmitters, and for the cases with and without defect.

We are dealing with two defect parameters: the defect diameter and its depth below the specimen surface. Fig. 4

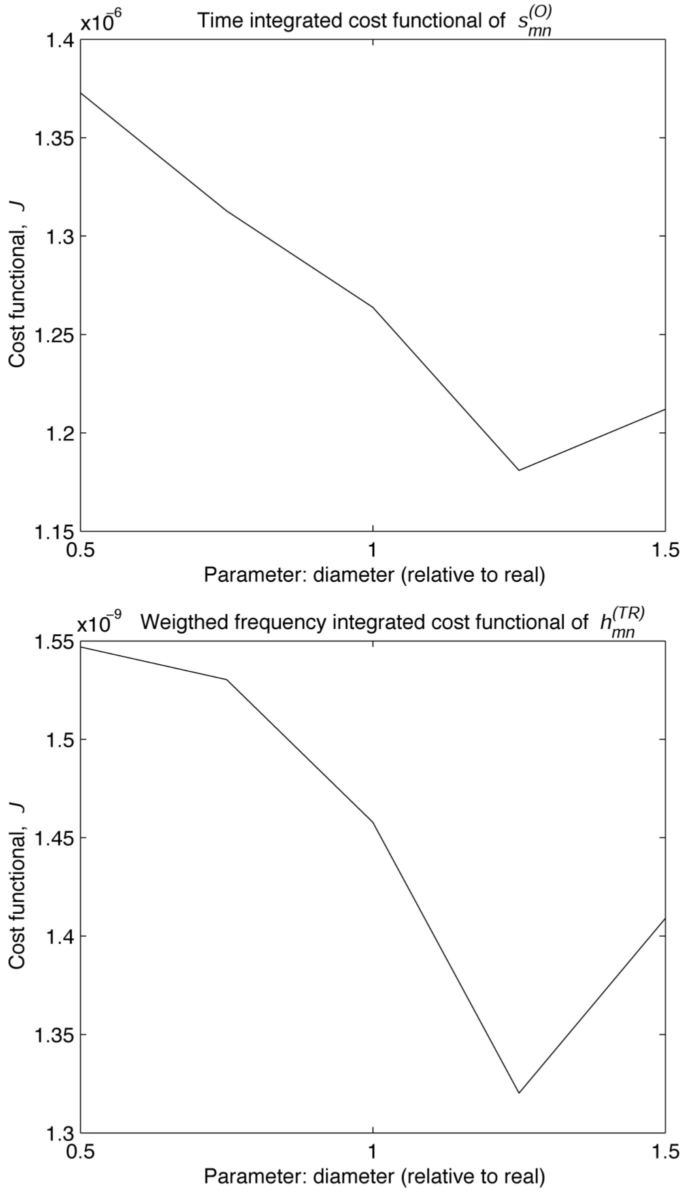

Fig. 4. Variation of the cost functional with respect to the first defect parameter: diameter. Two versions of the definition of J.

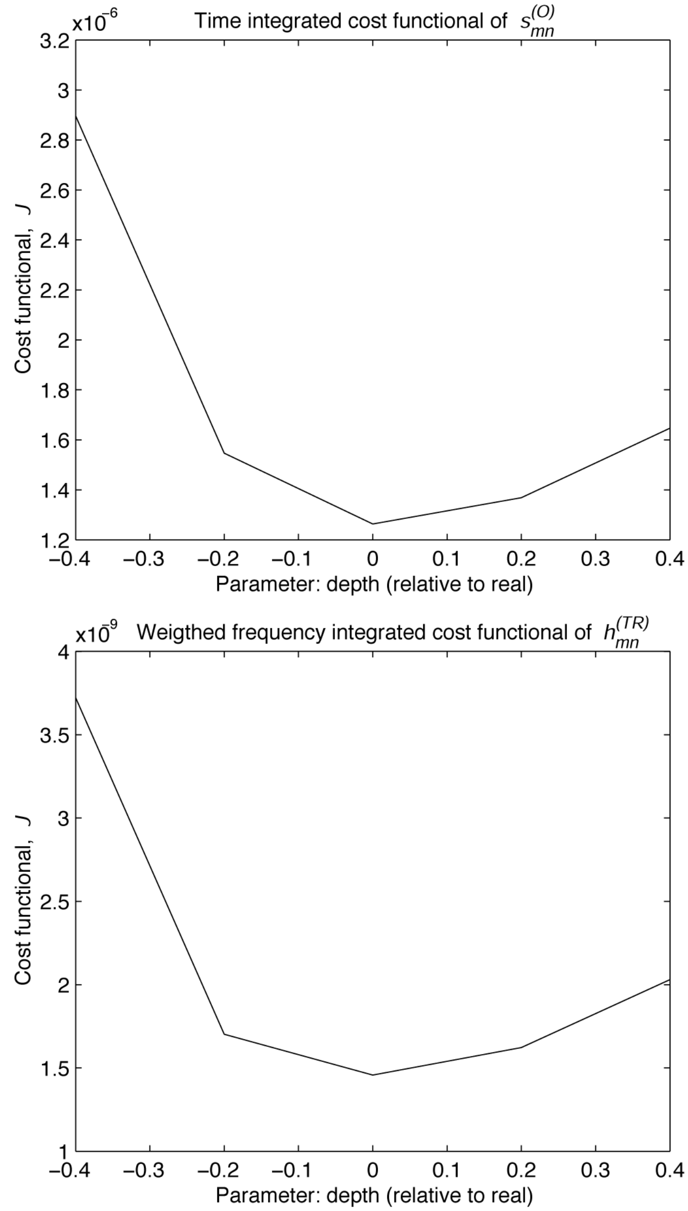

Fig. 5. Variation of the cost functional with respect to the second defect parameter: depth. Two versions of the definition of J.

shows the cost functional J, defined in terms of either $s_{mn}^{(O)}$ or $h_{mn}^{(TR)}$, as a function of the diameter and the depth. In both cases, the cost functional shows its minimum value when the defect parameters reach their real values, i.e., when the normalized diameter ($D_{\mathrm{predicted}}/D_{\mathrm{real}}$) approaches unity and when the normalized depth ($d_{\mathrm{predicted}} - d_{\mathrm{real}}/d_{\mathrm{real}}$) reaches zero.

It can be observed that the variation due to the diameter variation is less sensitive. This is due to the fact that the range of J values (max-to-min ratio of approximately 1.2 to 1) is smaller than that for the depth, Fig. 5, which is approximately 2.5 to 1. From this observation, we can say that source errors affect the predicted values. As a consequence, the predicted value of the diameter is distorted by 25% as opposed to the correct prediction of the depth. This distortion is probably explained by the inaccuracy in the synthetic signal compared to the real one, in addition to the masking of the wave reflected from the defect below the predominant surface wave.

It is easy to observe that the variation of depth makes more contribution to the signals than that of diameter. When comparing the two functionals (based on $h_{mn}^{(TR)}$ and $s_{mn}^{(O)}$), the function of the former indicates better sensitivity, as the depth parameter ratio is 2.5:1 whereas that of the latter is 1.2 to 1.

V. Conclusions

The second part of the proposed model-based method analyzes the signals obtained from an array of ultrasonic transmitters and receivers. Our inversion procedure is an iterative method that minimizes the difference between the measured and the synthesized signals. In the first part, the model is implemented and two calibration methods are developed.

The inversion procedure makes the following contributions: (a) The inversion procedure can effectively deal with the predominance of surface waves that can possibly interfere with the echoes reflected off the actual defect. (b) The procedure deals with noise problems by normalization and parameterization of the signals without losing the signal fidelity. (c) The robustness property provided by the parametrization technique is gained at the compromise of allowing only simple geometries of the defect.

It is straightforward to modify the parametrization to account for more complex geometries as well as multiple defects. In particular, the case of straight or curved cracks with any orientation is implemented in the used boundary element code, as well as the case of inclusions. Other types of defects can be implemented by modifying this code, and using the same inverse procedure.

References

[1] I. A. Viktorov, *Rayleigh and Lamb Waves.* New York: Plenum Press, 1967.

[2] G. F. Miller and H. Pursey, "The field and radiation impedance of mechanical radiators on the free surface of a semi-infinite isotropic solid," in *Proc. Royal Soc. London, Series A: Math. Phys. Sci.*, vol. 223, no. 1155, May 1954, pp. 521–541.

[3] Y. H. Pao and C. C. Mow, *Diffraction of Elastic Waves and Dynamic Stress Concentrations.* New York: Crane, Russak, 1973.

[4] K. F. Graff, *Wave Motion in Elastic Solids.* Mineola, NY: Dover Publications, 1975.

[5] S. C. Wooh and I. M. Daniel, "Three dimensional ultrasonic imaging of defects and damage in composite materials," *Mater. Eval.*, vol. 52, no. 10, pp. 1199–1206, 1994.

[6] A. Boström and H. Wirdelius, "Ultrasonic probe modeling and nondestructive crack detection," *J. Acoust. Soc. Amer.*, vol. 97, pp. 2836–2848, 1995.

[7] A. Boström, G. Johansson, and P. Olsson, "On the derivation of a hierarchy of dynamic equations for a homogeneous, isotropic, elastic plate," *Int. J. Solids Struct.*, vol. 38, pp. 2487–2501, 2001.

[8] H. Wirdelius, "An optimization technique for inverse crack detection," *Comm. Div. Mech*, vol. 11, Göteborg, Sweden: Div. of Mechanics, CTH, 1994.

[9] L. M. Bezerra and S. Saigal, "A boundary element formulation for the inverse elastostatics problem (iesp) of flaw detection," *Int. J. Numer. Methods Eng.*, vol. 36, pp. 2189–2202, 1993.

[10] S. C. Mellings and M. H. Aliabadi, "Flaw identification using the boundary element method," *Int. J. Numer. Methods Eng.*, vol. 38, pp. 399–419, 1995.

[11] Z. Yao and B. Gong, "Defect identification using boundary element methods of elastostatics," in *Inverse Problems in Engineering Mechanics.* M. Tanaka, H. D. Bui, M. Bonnet, H. Maigre, E. Luzzato, and M. Reynier, Eds. Rotterdam: Balkema Pub., 1994.

[12] M. Bonnet, *Boundary Integral Equation Methods for Solids and Fluids.* Chichester, UK: John Wiley and Sons, 1995.

[13] T. Burczynski, J. H. Kane, and C. Balakrishna, "Shape design sensitivity analysis via material derivative-adjoint variable technique for 3-D and 2-D curved boundary elements," *Int. J. Numer. Methods Eng.*, vol. 38, pp. 2839–2866, 1995.

[14] G. E. Stavroulakis, *Inverse and Crack Identification Problems in Engineering.* Dordrecht, Boston, London: Kluwer Academic Publishers, 2001.

[15] R. Gallego and J. Suárez, "Numerical solution of the variation boundary integral equation for inverse problems," *Int. J. Numer. Methods Eng.*, vol. 49, pp. 501–518, Oct. 2000.

[16] G. Rus and R. Gallego, "Solution of identification inverse problems by a sensitivity boundary integral equation," in *Proc. ECCOMAS2000*, E. Oñate, G. Bugeda, and B. Suárez, Eds. 2000.

[17] F. J. Suárez, "Aplicación del método de los elementos de contorno a la resulución del problema inverso en elastodinámica," Ph.D. dissertation, Universidad de Granada, E.T.S.I. Caminos, C. y. P., Nov. 1998.

[18] P. L. Liu and C. C. Chen, "Parametric identification of truss structures by using transient response," *J. Sound Vibr.*, vol. 191, no. 2, pp. 273–287, 1996.

[19] A. Tarantola and B. Valette, "Inverse problems—Quest for information," *J. Geophys.*, vol. 50, pp. 159–170, 1982.

[20] D. Bernal, "Load vectors for damage localization," *J. Eng. Mech.*, vol. 128, no. 1, pp. 7–14, Jan. 2002.

[21] S.-C. Wooh, A. Clay, and C. Wei, "Ultrasonic phased array transducers for nondestructive evaluation of steel structures," in *Proc. Spring Conf. Exp. Appl. Mech., Soc. Exp. Mech., Ed.*, 1997, pp. 1–2.

[22] S.-C. Wooh and Y. Shi, "Optimization of ultrasonic phased arrays," *Rev. Progr. Quant. Nondestruct. Eval.*, vol. 17, pp. 883–890, 1998.

[23] G. Rus and R. Gallego, "Boundary integral equation for inclusion and cavity shape sensitivity in harmonic elastodynamics," *Eng. Anal. Boundary Elements*, vol. 25, pp. 77–91, 2005.

[24] G. Rus and R. Gallego, "Solution of identification inverse problems in elastodynamics using semi-analytical sensitivity computation," *Eng. Anal. Boundary Elements*, vol. 31, no. 4, pp. 343–360, 2007.

[25] G. Rus and R. Gallego, "Optimization algorithms for identification inverse problems," in *Proc. 10th Int. Congr. CMEM2001*, B. Suárez, E. Oñate, and G. Bugeda, Eds. 2001.

[26] G. Rus, "Numerical methods for nondestructive identification of defects," Ph.D. dissertation, Universidad de Granada, E.T.S.I. Caminos, C. y. P., June 2001.

[27] G. Rus, S. Wooh, and R. Gallego, "Analysis and design of wedge transducers using the boundary element method," *J. Acoust. Soc. Amer.*, vol. 115, pp. 2919–2927, 2004.

Guillermo Rus received his Ph.D. degree in numerical methods for nondestructive identification of defects in 2001 at the University of Granada, Granada, Spain. He worked at the NDE Laboratory at the Massachusetts Institute of Technology, Cambridge, MA, as a Fulbright Postdoctoral Fellow during 2002–2003. He was also a visitor at the University College London (UK), Chalmers Technical University, Linkoping Institute of Technology (Sweden), Ecole Polytechnique (France), and the University of Alicante and the University Miguel Hernández (Spain), supported by different grants. He teaches structural mechanics as an associate professor at the University of Granada, where he is also promoting the Nondestructive Evaluation Laboratory. Dr. Rus is the recipient of several prestigious awards, including the Juan Carlos Simó for young researchers in numerical methods (SEMNI), and is a Fellow of the Wessex Institute of Great Britain.

Shi-Chang Wooh is President of Remos Technologies, Inc. He obtained his Ph.D. degree in theoretical and applied mechanics from Northwestern University, Evanston, Illinois. Before founding Remos Technologies, he was an Esther and Harold E. Edgerton Associate Professor at the Massachusetts Institute of Technology. His research areas encompass a broad spectrum of mechanics, including wave propagation and ultrasonics, nondestructive evaluation, sensor technology, composite materials and structures as well as embedded systems design and applications. Dr. Wooh is the recipient of several prestigious awards, including the Esther and Harold E. Edgerton Development Chair and NSF CAREER award. He has coauthored more than 140 technical papers.

Rafael Gallego is Professor and Head of the Department of Structural Mechanics of the University of Granada. He graduated and obtained his Ph.D. degree at the University of Sevilla, Sevilla, Spain, and was a Fulbright Postdoctoral Fellow at Brown University, Providence, RI. His active research field focuses on the application of the boundary element method in damage evaluation and characterization of advanced materials, particularly using topological and geometrical sensitivity. He is co-author of seven books and more than 40 papers in international journals.